Regulation of plasminogen activation: a role for melanotransferrin (p97) in cell migration. Blood 2003;102:1723–31.

Jin H, Zhang C, Zwahlen M, von Feilitzen K, Karlsson M, Shi M, et al. Systematic transcriptional analysis of human cell lines for gene expression landscape and tumor representation. Nat Commun 2023;14:5417.

Jin X, Demere Z, Nair K, Ali A, Ferraro GB, Natoli T, et al. A metastasis map of human cancer cell lines. Nature 2020;588:331–6.

Mazahreh R, Mason ML, Gosink JJ, Olson DJ, Thurman R, Hale C, et al. SGN-CD228A is an investigational CD228-directed antibody-drug conjugate with potent antitumor activity across a wide spectrum of preclinical solid tumor models. Mol Cancer Ther 2023;22:421–34.

Rolland Y, Demeule M, Béliveau R. Melanotransferrin stimulates t-PA-dependent activation of plasminogen in endothelial cells leading to cell detachment. Biochim Biophys Acta 2006;1763:393–401.

Rolland Y, Demeule M, Fenart L, Béliveau R. Inhibition of melanoma brain metastasis by targeting melanotransferrin at the cell surface. Pigment Cell Melanoma Res 2009;22:86–98.

Rolland Y, Demeule M, Michaud-Levesque J, Béliveau R. Inhibition of tumor growth by a truncated and soluble form of melanotransferrin. Exp Cell Res 2007;313:2910–9.

Singh CSB, Eyford BA, Abraham T, Munro L, Choi KB, Okon M, et al. Discovery of a highly conserved peptide in the iron transporter melanotransferrin that traverses an intact blood brain barrier and localizes in neural cells. Front Neurosci 2021;15:596976.

Suryo Rahmanto Y, Dunn LL, Richardson DR. The melanoma tumor antigen, melanotransferrin (p97): a 25-year hallmark–from iron metabolism to tumorigenesis. Oncogene 2007;26:6113–24.

Topically Applied N,N-Dimethylglycine Sodium Salt Enhances Human Skin Blood Flow by Inducing Endothelial Nitric Oxide Release

JID Open

Journal of Investigative Dermatology (2024) **144,** 2823–2827; doi:10.1016/j.jid.2024.04.019

TO THE EDITOR

N,N-dimethylglycine (DMG), being part of the endogenous homocysteine pathway, and its sodium salt (DMG-Na) have been widely used in animal husbandry to increase feed/weight ratio, induce fattening, or boost physical performance and were also approved as a safe nonfuel food supplement for humans (Cupp and Tracy, 2003; Greene et al, 1996; Kalmar et al, 2014; Prola et al, 2013). DMG and DMG-Na were also shown to support tissue and cellular functions, for example, by improving antioxidant capacities and oxygen utilization, promoting tissue regeneration, and enhancing immune response/defense (Bai et al, 2016; Feng et al, 2018; Graber et al, 1981; Kalmar et al, 2014).

With respect to the skin, we have recently shown that DMG-Na promoted the proliferation and migration of human epidermal keratinocytes and upregulated the synthesis of several GFs. Furthermore, DMG-Na exerted robust anti-inflammatory and antioxidant effects in various human keratinocyte in vitro models of allergic contact dermatitis, psoriasis, and UVB irradiation–induced solar dermatitis. We also found that these cellular actions of DMG-Na were accompanied by elevation of intracellular calcium ion concentration ($[Ca^{2+}]_i$) (Lendvai et al, 2023).

Because increase in $[Ca^{2+}]_i$ plays a crucial role in the regulation of skin microcirculation (Cracowski and Roustit, 2020; Zhao et al, 2015) by activating endothelial nitric oxide synthase (eNOS) and inducing nitric oxide (NO) production, we aimed to uncover whether DMG-Na can induce endothelium-derived NO release. In the first part of our study, we therefore employed various cellular and molecular techniques (Supplementary Materials and Methods provides details) and measured the effects of DMG-Na in vitro on primary human dermal microvascular endothelial cells (HDMECs).

First, we measured the effects of DMG-Na on the $[Ca^{2+}]_i$ of HDMECs. As detected by fluo-4 acetoxymethyl–based microfluorimetry, in normal (1.8 mM) calcium ion–containing medium, DMG-Na elevated the $[Ca^{2+}]_i$ of HDMECs in a dose-dependent manner; in this study, 0.02 and 0.05% of DMG-Na exerted statistically significant responses ($P < .0001$ in both cases) compared with the control (Figure 1a and c). In contrast, DMG-Na was completely ineffective to increase $[Ca^{2+}]_i$ in a calcium ion–free medium supplemented with 5 mM EDTA (Figure 1b and c). The fact that DMG-Na was able to increase $[Ca^{2+}]_i$ only in the presence of extracellular calcium ion suggests that DMG-Na induced calcium influx to HDMECs from the extracellular space.

Next, we assessed whether DMG-Na influences eNOS expression of HDMECs. As shown by semiquantitative immunocytochemistry, DMG-Na appeared to upregulate the expression of eNOS after 24 hours of treatment (Figure 1d). This was quantitatively verified by western blotting, suggesting that DMG-Na indeed dose-dependently and, in the case of 0.05% DMG-Na, statistically significantly ($P = .0189$) increased the protein level of eNOS compared with the control (Figure 1e and f). In addition, DMG-Na treatment also significantly upregulated the level of Ser1177-phosphorylated eNOS, which was

Abbreviations: $[Ca^{2+}]_i$, intracellular calcium ion concentration; DMG, N,N-dimethylglycine; DMG-Na, N,N-dimethylglycine sodium salt; eNOS, endothelial nitric oxide synthase; HDMEC, human dermal microvascular endothelial cell; NO, nitric oxide

Accepted manuscript published online 24 May 2024; corrected proof published online 12 June 2024

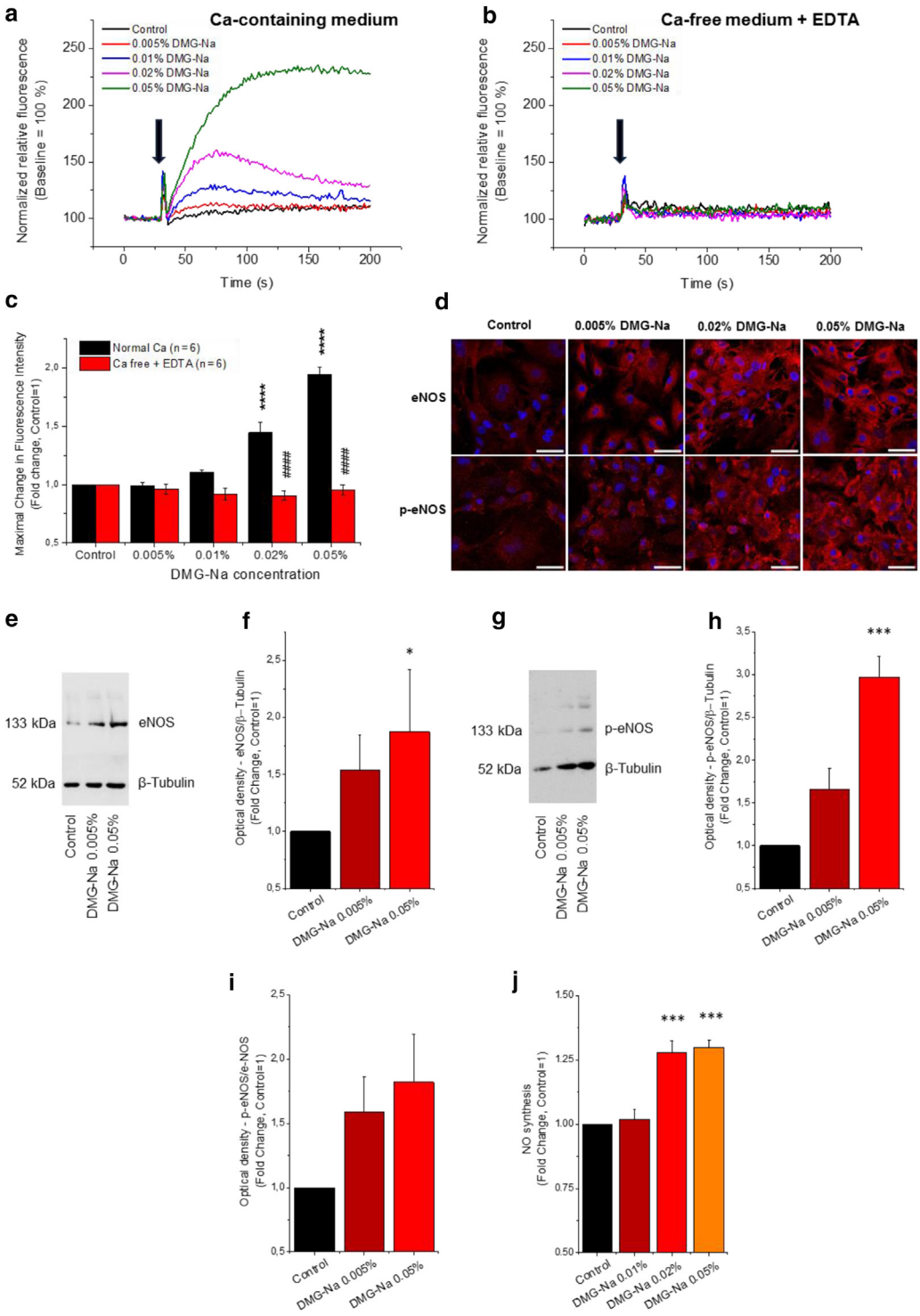

Figure 1. Effects of DMG-Na on various biological functions of HDMECs in vitro. (**a**, **b**) Representative microfluorimetric Ca^{2+} measurements recorded on Fluo-4 AM–loaded HDMECs measured in (**a**) 1.8 mM Ca^{2+}-containing medium and (**b**) Ca^{2+}-free medium supplemented with 5 mM EDTA (6 independent experiments each). The arrows indicate the application of various concentrations of DMG-Na and control. (**c**) Statistical analysis of maximal amplitudes of $[Ca^{2+}]_i$ elevations induced by the various concentrations of DMG-Na in the 2 media, shown as fold change values (mean ± SEM, n = 6 independent experiments) when normalized to the respective controls. For *P*-values, * marks the statistical difference compared with the respective vehicle controls (****$P <$ .0001), whereas # marks statistical differences between measurements in the 2 media using 2-way ANOVA with Tukey's posthoc test ($^{\#\#\#\#}P <$ .0001). (**d**) Representative immunofluorescent labeling of eNOS and the Ser1177 phosphorylated form of eNOS (p-eNOS) in HDMECs (of 3 independent experiments each) treated with various concentrations of DMG-Na. eNOS and p-eNOS were labeled with red, whereas nuclei were counterstained by DAPI (blue). Bar = 50 μm. (**e**) Representative western blot immunolabeling (of 4 independent experiments) of eNOS and β-tubulin in HDMECs treated with various concentrations of DMG-Na. (**f**) Statistical analysis of optical density measurements on immunoblots. Relative eNOS/β-tubulin values (mean ± SEM, n = 4 independent experiments) are shown as fold change when normalized to the respective vehicle controls. For *P*-values, * marks the statistical difference compared with the control as determined by Kruskal–Wallis with Dunn's posthoc test (*$P <$ .05). (**g**) Representative western blot immunolabeling (of 4 independent experiments) of

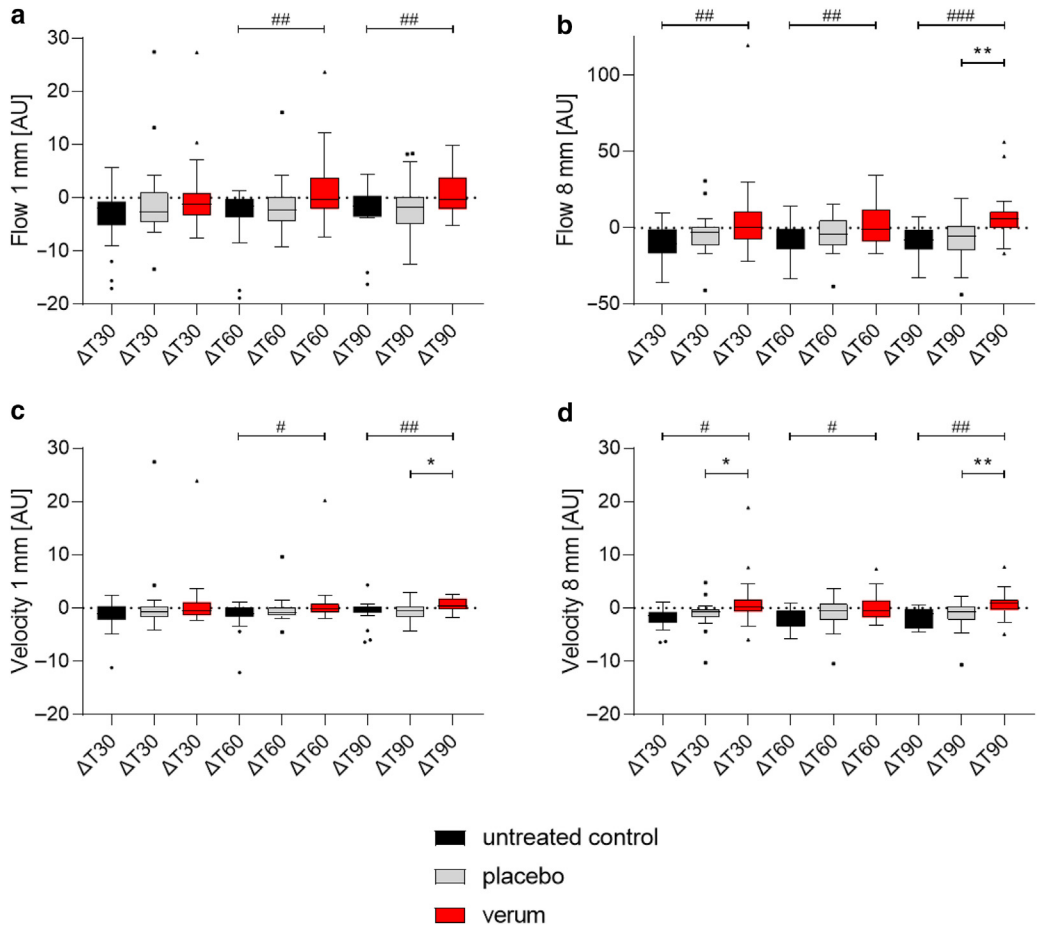

Figure 2. Effects of DMG-Na on the microcirculation of human skin in vivo. (**a**, **b**) Dermal microcirculation measured through blood flow at (**a**) 1-mm and (**b**) 8-mm skin depth upon indicated treatments (untreated control, placebo, or verum). **(c, d)** Dermal microcirculation measured through blood velocity at (**c**) 1-mm and (**d**) 8-mm skin depth upon indicated treatments (untreated control, placebo, or verum). Box and whisker plots (Tukey method) showing the median, quartiles, and extreme values for T30 to T0 differences (ΔT30), T60 to T0 differences (ΔT60), and T90 to T0 differences (ΔT90) of blood flow in AUs. Effects measured in the verum group were compared with those measured in both the untreated control and placebo groups, and *P*-values calculated by Wilcoxon signed rank test are shown as follows: $*P < .05$ and $**P < .01$ significant difference compared with the placebo and $\#P < .05$ and $\#\#P < .01$ significant difference compared with the untreated control. AU, arbitrary unit; DMG-Na, N,N-dimethylglycine sodium salt; T0, time 0 minute; T30, time 30 minutes; T60, time 60 minutes; T90, time 90 minutes.

proven by complementary immunocytochemistry (Figure 1d) and western blotting, where the effect of 0.05% DMG-Na was found to be statistically significant ($P = .0001$) compared with that of control (Figure 1g and h). Furthermore, as defined by optical density analysis of the western blot data, DMG-Na treatment also increased the phosphorylated eNOS/eNOS ratio (although this effect did not reach statistical significance) (Figure 1i). These data collectively argue that DMG-Na treatment of HDMECs activated the eNOS enzyme.

Finally, we measured the effect of DMG-Na on NO synthesis of HDMECs. Using 4-amino-5-methylamino-2′,7′-difluororescein diacetate–based microfluorimetry, we found that 0.02 and 0.05% DMG-Na statistically significantly ($P = .0002$ and $P = .0001$, respectively) increased cellular NO production compared with the control (Figure 1j).

Despite the necessity to perform further in-depth mechanistic studies, these in vitro data unambiguously showed that DMG-Na engages the $\uparrow[Ca^{2+}]_i$ – eNOS activation – ↑NO synthesis triad. On the basis of this, one may hypothesize that DMG-Na, when applied topically to the skin, may

Ser 1177 p-eNOS and β-tubulin in HDMECs treated with various concentrations of DMG-Na. (**h**) Statistical analysis of optical density measurements on immunoblots. Relative p-eNOS/β-tubulin values (mean ± SEM, n = 4 independent experiments) are shown as fold change when normalized to the respective vehicle controls. For *P*-values, *** marks the statistical difference compared with the control as determined by 1-way ANOVA followed by Dunnett's posthoc test ($***P = .0001$). (**i**) Statistical analysis of optical density measurements on immunoblots. Relative p-eNOS/e-NOS values (mean ± SEM, n = 4 independent experiments) are shown as fold change when normalized to respective β-tubulin values and to the respective vehicle controls. (**j**) Statistical analysis of microfluorimetric measurement of NO synthesis. Values (mean ± SEM, n = 4 independent experiments) are shown as fold change when normalized to the respective controls. For *P*-values, * marks the statistical difference compared with the control using 1-way ANOVA with Dunnett's posthoc test ($***P < .001$). AM, acetoxymethyl; Ca^{2+}, calicium ion; $[Ca^{2+}]_i$, intracellular calcium ion concentration; DMG-Na, N,N-dimethylglycine sodium salt; eNOS, endothelial nitric oxide synthase; HDMEC, human dermal microvascular endothelial cell; NO, nitric oxide; p-eNOS, phosphorylated endothelial nitric oxide synthase.

induce endothelium-dependent vasodilation and boost skin microcirculation.

To probe this idea, we designed a monocentric, single-blinded, randomized, placebo-controlled human in vivo study in which the effects of a topically applied 1% DMG-Na gel were assessed on the microcirculation parameters, skin blood flow (the volume of blood movement over time), and skin blood flow velocity (the rate of blood movement over a distance) (Supplementary Materials and Methods provides detailed design). Human subjects provided written, informed consent prior to the study. The study design for noninvasive surveys was approved by the Ethics Committee of the Witten/Herdecke University (Witten, Germany).

As measured by the Doppler effect–based O2C system (Supplementary Materials and Methods), at 1-mm skin depth, DMG-Na slightly increased blood flow already T30 minutes after topical application, which reached statistically significant flow rate increase at T60 minutes ($P = .0073$) and T90 minutes ($P = .0027$) compared with that at the untreated control area (Figure 2a and Supplementary Table S1). At 8-mm skin depth, the effect of DMG-Na was even more profound. Namely, statistically significant augmentation of blood flow was found T90 minutes ($P = .0083$) after treatment compared with that at placebo-treated test area, whereas compared with the untreated control area, statistical significance was reached in favor of the DMG-Na–treated test area at all time points (T30 minutes: $P = .0014$, T60 minutes: $P = .0032$, T90 minutes: $P = .0002$) (Figure 2b and Supplementary Table S2).

Besides the blood flow rate, topically applied 1% DMG-Na also increased dermal blood velocity at both skin depths measured. At 1 mm, statistical significance was reached at T90 minutes ($P = .0266$) compared with that at the placebo-tested area, whereas compared with the untreated control, statistical significance was observed at T60 ($P = .0215$) and T90 ($P = .0023$) minutes (Figure 2c and Supplementary Table S3). Furthermore, at 8-mm skin depth, the velocity-increasing effect of topical DMG-Na was statistically significant at T30 ($P = .0362$) and T90 ($P = .0042$) minutes compared with that of the placebo, whereas compared with the untreated area, statistical significance was reached at all time points (T30 minutes: $P = .0289$, T60 minutes: $P = .0152$, T90 minutes: $P = .0024$) (Figure 2d and Supplementary Table S4).

Notably, over the course of this in vivo study, an increase in microcirculation was observed for all volunteers (1 subject even showed a slight temporary red blotchiness of the skin about 60 minutes after application of the verum product), which correlates with the increase in microcirculation. However, no undesirable effects such as, for example, itching, stinging, feeling of tension, or any other discomfort were observed.

Taken together, these pioneer data provide, to our knowledge, previously unreported human in vivo evidence that topical DMG-Na robustly increases the intensity of dermal blood flow by penetrating into deeper cutaneous layers. Furthermore, our complementary in vitro experiments clearly show that the effects of DMG-Na mentioned earlier are most probably due to its actions on HDMECs, which in turn induces endothelium-derived, NO-dependent vasodilation (a short summary on the safety of DMG-Na can be found in Supplementary Discussion).

Thus, our in vivo and in vitro findings collectively suggest that DMG-Na might be highly promising active in conditions such as skin aging, atrophy, acute or chronic wounds, hair loss of any kind, and various dermatitis, in which the beneficial effects of DMG-Na to promote epidermal proliferation, regeneration, and repair; to augment skin blood flow and velocity; and to exert protective functions could be of great impact. Further clinical studies are now warranted to explore the enormous application potential of DMG-Na in multiple human skin pathologies (we have recently completed 3 human trials with DMG-Na containing topical formulations [tonic or shampoo] on a total of 462 subjects suffering from male- and female-pattern hair loss). Further information on the outcome of these studies can be found in Supplementary Discussion).

DATA AVAILABILITY STATEMENT

No large datasets were generated or analyzed during this study.

KEYWORDS

Human dermal microvascular endothelial cells; Microcirculation; Nitric oxide; N,N-dimethylglycine sodium salt; Skin blood flow

ORCIDs

Gabriella Béke: http://orcid.org/0000-0003-3113-2287
Alexandra Lendvai: http://orcid.org/0000-0002-6530-6356
Erika Hollósi: http://orcid.org/0000-0002-1495-4863
Nicole Braun: http://orcid.org/my-orcid?orcid=0000-0001-5925-8485
Carmen Theek: http://orcid.org/0009-0006-7360-0105
Judit Kállai: http://orcid.org/0000-0002-7373-1459
Árpád Lányi: http://orcid.org/0000-0003-2265-4235
Maike Becker: http://orcid.org/0000-0001-7650-1969
Jörn Michael Völker: http://orcid.org/0000-0002-2407-2557
Erik Schulze zur Wiesche: http://orcid.org/0000-0003-0890-1666
Attila Bácsi: http://orcid.org/0000-0002-2311-2975
Tamás Bíró: http://orcid.org/0000-0002-3770-6221
Johanna Mihály: http://orcid.org/0000-0002-5499-750X

CONFLICT OF INTEREST

The authors state no conflict of interest.

ACKNOWLEDGMENTS

This study was supported by Dr. August Wolff GmbH & Co. KG Arzneimittel (Bielefeld, Germany) (III/1/2022) and by PD NKFIH-125057 for JM. JM is a recipient of the János Bolyai research scholarship of the Hungarian Academy of Sciences (BO/00481/17/5). Publication of the study was supported by the University of Debrecen Program for Scientific Publication.

AUTHOR CONTRIBUTIONS

Conceptualization: NB, MB, JMV, ESzW, AB, TB, JM; Methodology: GB, AL, EH, NB, CT, JK, ÁL; Project Administration: GB; EH; Supervision: NB, ÁL, MB, JMV, ESzW, TB, JM; Visualization: GB, NB, TB, JM; Writing - Original Draft Preparation: NB, TB, JM; Writing - Review and Editing: GB, AL, NB, CT, ÁL, MB, JMV, ESzW, AB, TB, JM

Gabriella Béke[1], Alexandra Lendvai[1,2], Erika Hollósi[1], Nicole Braun[3], Carmen Theek[4], Judit Kállai[1], Árpád Lányi[1], Maike Becker[5], Jörn Michael Völker[5], Erik Schulze zur Wiesche[5,6], Attila Bácsi[1,7], Tamás Bíró[1] and Johanna Mihály[1,]*

[1]*Department of Immunology, Faculty of Medicine, University of Debrecen, Debrecen, Hungary;* [2]*Gyula Petrányi Doctoral School of Clinical Immunology and Allergology, University of Debrecen, Debrecen, Hungary;* [3]*Eurofins DermaTronnier GmbH, Institute for*

Experimental Dermatology, Witten/Herdecke University, Witten, Germany; [4]*Carmen Theek, CTS, Witten, Germany;* [5]*Dr. Kurt Wolff GmbH & Co. KG, Bielefeld, Germany;* [6]*Dr. August Wolff GmbH & Co. KG Arzneimittel, Bielefeld, Germany; and* [7]*HUN-REN-UD Allergology Research Group, Debrecen, Hungary*
[*]*Corresponding author e-mail: johanna@med.unideb.hu*

SUPPLEMENTARY MATERIAL

Supplementary material is linked to the online version of the paper at www.jidonline.org, and at https://doi.org/10.1016/j.jid.2024.04.019.

REFERENCES

Bai K, Xu W, Zhang J, Kou T, Niu Y, Wan X, et al. Assessment of free radical scavenging activity of dimethylglycine sodium salt and its role in providing protection against lipopolysaccharide-induced oxidative stress in mice. PLoS One 2016;11:e0155393.

Cracowski JL, Roustit M. Human skin microcirculation. Compr Physiol 2020;10:1105–54.

Cupp MJ, Tracy TS. Dimethylglycine (N,N-dimethylglycine). In: Cupp MJ, Tracy TS, editors. Dietary supplements: toxicology and Clinical Pharmacology. Totowa: Humana Press; 2003. p. 149–60.

Feng C, Bai K, Wang A, Ge X, Zhao Y, Zhang L, et al. Effects of dimethylglycine sodium salt supplementation on growth performance, hepatic antioxidant capacity, and mitochondria-related gene expression in weanling piglets born with low birth weight1. J Anim Sci 2018;96:3791–803.

Graber CD, Goust JM, Glassman AD, Kendall R, Loadholt CB. Immunomodulating properties of dimethylglycine in humans. J Infect Dis 1981;143:101–5.

Greene HM, Wickler SJ, Bray RE, Burrill MJ, London C. The effect of N,N-dimethylglycine on athletic performance at altitude in horses and mules. Pferdeheilkunde 1996;12:499–501.

Kalmar ID, Verstegen MWA, Vanrompay D, Maenner K, Zentek J, Iben C, et al. Efficacy of dimethylglycine as a feed additive to improve broiler production. Livest Sci 2014;164:81–6.

Lendvai A, Béke G, Hollósi E, Becker M, Völker JM, Schulze Zur Wiesche E, et al. N,N-dimethylglycine sodium salt exerts marked anti-inflammatory effects in various dermatitis models and activates human epidermal keratinocytes by increasing proliferation, migration, and growth factor release. Int J Mol Sci 2023;24:11264.

Prola L, Nery J, Lauwaerts A, Bianchi C, Sterpone L, De Marco M, et al. Effects of N,N-dimethylglycine sodium salt on apparent digestibility, vitamin E absorption, and serum proteins in broiler chickens fed a high- or low-fat diet. Poult Sci 2013;92:1221–6.

Zhao Y, Vanhoutte PM, Leung SW. Vascular nitric oxide: beyond eNOS. J Pharmacol Sci 2015;129:83–94.

SUPPLEMENTARY DISCUSSION

Safety of N,N-dimethylglycine

N,N-dimethylglycine (DMG) is an intermediate of the endogenous choline and betaine metabolism in humans and can be considered as a ubiquitous compound being present in most human body tissues and/or body fluids. The DMG background level reported in plasma or serum of humans is in the range of 0.9–16.2 μM (Swierczynski et al, 2015).

DMG used for topical treatment is expected to have a consequently low risk for high systemic exposure. Considering that (i) DMG is an endogenous intermediate of the choline and betaine metabolism (ii) being present in many tissues, including the skin, as well as (iii) having broad plasma levels, it is expected that generally low total daily dermal use of DMG will not lead to a significant increase in DMG background levels in plasma. Furthermore, as mentioned in the main text, DMG and its sodium salt have been widely used in animal husbandry to increase feed/weight ratio, induce fattening, or boost physical performance and were also approved as a safe nonfuel food supplement for humans (Cupp and Tracy, 2003; Greene et al, 1996; Kalmar et al, 2014; Prola et al, 2013). Additional published clinical studies in adult subjects after oral use of DMG at significantly higher doses than the topical treatment also showed no negative impact or adverse clinical signs related to safety pharmacology (Gascon et al, 1989; Wolfsegger et al, 2021).

Finally, it is noteworthy that the median lethal dose was considered to be 5400 mg/kg (95% confidential limit = 4500–6400 mg/kg) for male and female rats, specifically, 5800 mg/kg (95% confidential limit = 5100–6600 mg/kg) for males and 3900 mg/kg (95% confidential limit = 3000–5000 mg/kg) for females, when Crl:CD BR male and female rats were treated with DMG hyrogen chloride orally by gavage (Kendall and Glaza, 1982).

Completed human trials with DMG sodium salt containing topical formulations against male- and female-pattern hair loss

Pattern hair loss is the most common type of hair loss in both men and women, characterized by the miniaturization and shortening of the anagen growth phase of affected hair follicles. Several influence factors have been described to impair healthy hair growth such as hormonal imbalances, stress, microinflammation, and improper nutrition supply (Natarelli et al, 2023). Early studies have already shown that subcutaneous blood flow is reduced in male-pattern hair loss (Klemp et al, 1984), giving rise to the potential of vasodilators, such as minoxidil, to reduce hair loss.

We have completed 3 independent double-blind, randomized, placebo-controlled human trials with DMG sodium salt (DMG-Na) and caffeine-containing topical formulations (tonic or shampoo) on a total of 462 subjects suffering from male- or female-pattern hair loss (Schulze zur Wiesche et al, 2023). Products (verum or placebo) were applied daily over a period of 6 months. Hair loss parameters were significantly reduced upon verum treatment compared with placebo, with no reported adverse events. All topical formulations were considered to have a good skin compatibility (manuscripts are currently under review or in preparation for submission).

SUPPLEMENTARY MATERIALS AND METHODS

In vitro cell culture studies

Materials. DMG-Na (Eastman Enhanz) was obtained from Eastman Chemical Company. During the course of the in vitro experiments, owing to the limited availability of the cells, the following DMG-Na concentrations were assessed: 0.005, 0.01, 0.02, and 0.05% for microfluorimetric measurements of intracellular calcium ion (Ca^{2+}) concentration; 0.01, 0.02, and 0.05% for microfluorimetric measurements of nitric oxide; 0.005, 0.02, and 0.05% for immunocytochemistry; and 0.005 and 0.05% for western blotting.

Cell culturing. Adult human dermal microvascular endothelial cells (HDMECs) were purchased in 2023 from Lonza and cultured in EBM-2 Endothelial Cell Growth Basal Medium supplemented with EGM-2 MV Microvascular Endothelial SingleQuots Kit (both from Lonza) containing human epidermal GF, VEGF, R^3-IGF-1, ascorbic acid, hydrocortisone, human fibroblast GF-β, fetal bovine serum, and gentamicin/amphotericin B according to the manufacturer's instructions. HDMECs were initiated from 2 different female donors, and passages 4–8 were used for the experiments.

Microfluorimetric measurements of intracellular Ca^{2+} concentration. HDMECs were seeded in 96-well, black-well/clear-bottom plates (Greiner Bio-One) at a density of 15,000 cells per well in growth medium supplemented as described earlier and cultured at 37 °C for 24 hours. The cells were washed once with Hank's solution (normal buffer: 136.89 mM sodium chloride, 5.55 mM glucose, 5.36 mM potassium chloride, 4.17 mM sodium bicarbonate, 1.26 mM calcium chloride, 0.49 mM magnesium chloride × 6 dihydrogen monoxide, 0.34 mM disodium phosphate × 2 dihydrogen monoxide, 0.44 mM potassium dihydrogen phosphate, 0.24 mM magnesium sulfate × 7 dihydrogen monoxide, containing 2.5 mM of probenecid and 1% BSA, pH 7.2; Ca^{2+}-free EDTA-containing buffer: equimolar glucose substituted for calcium chloride and completed with 5 mM EDTA) and then loaded with the cytoplasmic calcium indicator 2 μM fluo-4 acetoxymethyl (Thermo Fisher Scientific) dissolved in either normal or in Ca^{2+}-free EDTA-containing Hank's balanced salt solution (100 μl per well) at 37 °C for 1 hour. The cells were washed with Ca^{2+}-containing (normal buffer) or Ca^{2+}-free (Ca^{2+}-free EDTA-containing buffer) Hank's solution (100 μl per well), and the plates were then placed into a FlexStation II^{384} Fluorescence Imaging Plate Reader (Molecular Devices), and changes in intracellular Ca^{2+} concentration (reflected by changes in fluorescence, λ_{EX} = 494 nm, λ_{EM} = 516 nm) induced by different DMG-Na concentrations (0.005, 0.01, 0.02, and 0.05%), along with vehicle control, were recorded in each well (during the measurement, cells in a given well were exposed to only 1 given concentration of the agent). For the analog graphs (Figure 1a and b), the fluorescence intensity values were normalized to the baseline fluorescence (regarded as 100%) recorded before the application of the agents. For the statistical analysis (Figure 1c), normalized fluorescence values obtained in the 6 independent experiments were pooled, and the maximal change in the fluorescence intensity induced by the

different DMG-Na concentrations was calculated and shown as fold change values compared with those of the control (regarded as 1) (Borbíró et al, 2011; Czifra et al, 2012; Lendvai et al, 2023; Szabó et al, 2020; Szöllősi et al, 2018).

Immunocytochemistry. HDMECs (5000 cells per 10 mm circular glass coverslips) treated with DMG-Na (0.005, 0.02, and 0.05%) were fixed in 1% paraformaldehyde (Merck KGaA) for 10 minutes at room temperature and after a washing step with PBS (Merck KGaA) post-fixed with −20 °C ethanol-acetic acid (2:1) for 5 minutes. Cells were permeabilized by 0.25% Triton X-100 in PBS for 10 minutes, blocked with Antibody Diluent (Thermo Fisher Scientific) for 30 minutes at room temperature and then incubated with anti-human endothelial nitric oxide synthase (eNOS) primary mouse antibody at 1:100 dilution (Abcam, number ab76198) or with anti-human phosphorylated eNOS Ser1177 primary rabbit antibody at 1:100 dilution (Abcam, number ab184154) at 4 °C overnight. After the appropriate washing step with PBS, for fluorescence staining, coverslips were incubated with Alexa Flour 568 goat anti-mouse IgG secondary antibody (Thermo Fisher Scientific, number A-11004) (for eNOS) or with Alexa Flour 568 goat anti-rabbit IgG secondary antibody (Thermo Fisher Scientific, number A-11011) (for phosphorylated eNOS), both at 1:500 dilution at room temperature for 45 minutes. Coverslips were washed with PBS, and nuclear counterstaining was carried out by DAPI (Merck KGaA) for 1 minute. After another washing step, cells on coverslips were mounted with Fluoromount-G (SouthernBiotech). Images were captured by a Nikon A1 confocal microscope and analyzed using the Image J Fiji software, version 2.9.0 (National Institutes of Health) (Borbíró et al, 2011; Czifra et al, 2012; Géczy et al, 2012; Lendvai et al, 2023; Szöllősi et al, 2018; Tóth et al, 2011, 2009).

Western blot. Cells were seeded in 6-well plates and treated with DMG-Na (0.005 and 0.05%) for 24 hours. After the treatment, cells were harvested in lysis buffer (30 mM Tris, pH 7.6, 140 mM sodium chloride, 5 mM EDTA, 50 mM sodium fluoride, 1 mM sodium orthovanadate) supplemented with protease inhibitors. After vigorous vortex and centrifugation, the protein contents of the samples were determined using Pierce BCA Protein Assay Kit (Thermo Fisher Scientific). Equal amounts of protein samples were subjected to 7.5% SDS-PAGE and transferred to nitrocellulose membranes (Bio-Rad Laboratories). The protein-binding nitrocellulose membranes were blocked with 5% skimmed milk in 1× Tris-buffered saline with 0.1% Tween 20 (TBST) for 1 hour at room temperature and then probed with a mouse monoclonal (M221) anti-eNOS primary antibody (Abcam, number ab76198) or a rabbit antiphosphorylated eNOS Ser1177 primary antibody (Abcam, number ab184154), both at dilution 1:1000 in 2.5% skimmed milk/1× TBST overnight at 4 °C. Membranes were washed 3 times in 1× TBST for 7 minutes and then incubated with horseradish peroxidase–labeled anti-mouse IgG secondary antibody (GE Healthcare, number NA931V) at dilution 1:5000 (for eNOS) or anti-rabbit IgG secondary antibody (GE Healthcare, number NA934W) at dilution 1:10,000 (for phosphorylated eNOS) in 1.5% skimmed milk/1× TBST for 45 minutes at room temperature. Bands were visualized by SuperSignal West enhanced chemiluminescence systems (Thermo Fisher Scientific) using a CCD-camera based imager, Azure c300 Gel Imaging System (Azure Biosystems). Densitometric analysis was performed using Azure Spot version 2.0.062 image analysis software. For optical density normalization, the membranes were reprobed using anti–β-tubulin primary antibody (Thermo Fisher Scientific, number PA5-86071) at dilution 1:10,000 in 2.5% skimmed milk/1× TBST, and as secondary antibody, anti-rabbit IgG horseradish peroxidase (GE Healthcare, number NA934V) at dilution 1:10,000 in 1.5% skimmed milk/1× TBST was used (Borbíró et al, 2011; Czifra et al, 2012; Géczy et al, 2012; Markovics et al, 2020; Szöllősi et al, 2018; Tóth et al, 2011, 2009).

Microfluorimetric measurements of nitric oxide. Dermal microvascular endothelial cells were seeded at a density of 15,000 cells per well in a black, clear-bottom, 96-well plate (Greiner Bio-One) and cultured in growth medium at 37 °C for 24 hours. Cells were then loaded with 5 μM 4-amino-5-methylamino-2′,7′-difluororescein diacetate in phenol red–free DMEM (both from Thermo Fisher Scientific) supplemented with 0.5% fetal bovine serum (Serana Europe GmbH) for 1 hour at 37 °C. HDMECs were washed to remove the excess probe, replaced with fresh medium, and then incubated for an additional 30 minutes at 37 °C to allow complete de-esterification of the intracellular diacetates. After incubation, cells were treated with DMG-Na (0.01, 0.02, and 0.05%), and fluorescence was measured at excitation/emission of 490/510 nm using a FlexStation II (Molecular Devices) fluorescence microplate reader (Nagy et al, 2004, 2003).

Statistical analysis. Graphs were plotted by OriginPro 8.6 software (OriginLab), and data were analyzed by GraphPad Prism, version 8.0.1, for Windows (GraphPad Software). For normally distributed data, 1-way ANOVA followed by Dunnett's posthoc test was performed. When data distribution was not normal, Kruskal–Wallis test with Dunn's multiple comparison test was used. In the case of intracellular calcium measurements, data were analyzed using 2-way ANOVA followed by Tukey's posthoc test.

In vivo human studies

Study design and test subjects. In this monocentric, single-blinded, randomized, placebo-controlled study to investigate the efficacy on dermal microcirculation, a total of 20 volunteers (16 female and 4 male) aged 18–30 years (Ø = 24.90 years) with healthy, normal skin type took part. Exclusion criteria were pregnancy and breast feeding, use of topical or systemic treatment during the previous weeks liable to interfere with the assessment of the cutaneous acceptability of the study product, subject having undergone a surgery under general anesthesia within the previous month, excessive exposure to sunlight or UV rays within the previous month, and enrollment in another clinical trial during the study period that could interfere with this study. Furthermore, participants were instructed not to apply any other similar product to the test areas 24 hours before study start; not to initiate a hormonal treatment nor change their usual hormonal treatment; and not to change lifestyle such as diet, smoking, and sport. The subjects were informed in detail about the aim and scope of the study; read the information sheets; and provided written, informed consent prior to study participation. The study design for noninvasive surveys was approved by the Ethics Committee of the Witten/Herdecke University (Witten, Germany) and was conducted according to the following guidelines: ICH TOPIC

E6 (R2)/Note for guidance on Good Clinical Practice − CPMP/ICH/135/95, November 2016; World Medical Association Declaration of Helsinki/Ethical Principles for Medical Research Involving Human Subjects - Helsinki Declaration (1964) and its successive updates; Regulation (EU) 2016/679 of the European Parliament and of the Council of 27 April 2016 on the protection of natural persons with regard to the processing of personal data and on the free movement of such data and repealing Directive 95/46/EC (General Data Protection Regulation); and Regulation (EC) No 1223/2009 of the European Parliament and of the Council of 30 November 2009 on cosmetic products (recast).

Formulations. In the human in vivo study, the following gel formulations were applied: DMG-Na (1%), aqua, poloxamer 407, alcohol, and citric acid for verum and sodium hydroxide, aqua, poloxamer 407, alcohol, and citric acid for placebo. Both formulations contained the same ingredient concentrations (except DMG-Na and sodium hydroxide) and were adjusted to pH 4.5-5. DMG-Na (Eastman Enhanz) was obtained from Eastman Chemical Company, and alcohol (96% ethanol) was obtained from Tereos France. Poloxamer 407 was obtained from BASF. Citric acid was obtained from S.A. Citrique Belge N.V.. Sodium hydroxide pellets were obtained from Merck KGaA.

Efficacy study. The O2C system (LEA Medizintechnik GmbH) was used to measure the short-term effects of the active DMG-Na on dermal blood flow and velocity between 0 and 90 minutes after a single application at 2 depths: 1 and 8 mm. The measurement of blood flow and velocity (arbitrary units) was determined by the frequency of light shifted by moving erythrocytes (the Doppler effect) (Berardesca et al, 2002; Braun et al, 2019; Walter et al, 2002).

The volunteers were asked to sit down, and the forearm remained in the same position during the entire experiment. Volunteers were not allowed to be in any way physically active during the measurement. All measurements were performed after an acclimatization period of 15−20 minutes at 22 °C under the same conditions. The measurements were performed on the volar forearm.

First, the baseline values on the volar forearm were determined before the application of the verum and placebo. Subsequently, the verum or placebo was applied, and the capillary blood flow and velocity were measured 30, 60, and 90 minutes after application. An untreated area served as control. The test areas on the inner forearm were chosen at random (left or right arm), where the control was always measured on the inner upper arm to exclude the measurement of effects of the verum. Data on microcirculation were recorded over 60 seconds (measurement every second) for each measurement time point.

All skin measurements were performed by Eurofins Derma Tronnier GmbH, Institute for Experimental Dermatology at the Witten/Herdecke University.

Statistical analysis. Descriptive summary statistics were calculated for the 2 parameters separately for 3 groups and for all 4 time points. Statistics comprise mean and median values, SD, and minimum and maximum. In addition, to capture the development over time, individual differences to baseline (pre−post difference) were determined, and the same summary statistics were provided.

To investigate the treatment effect (group comparisons for placebo versus actual treatment and untreated control versus actual treatment), the nonparametric Wilcoxon signed rank test was applied on an alpha level of 5% (2 sided), analyzing the pre−post differences from baseline. The analysis was performed on the observed values, that is, considering the individual differences from baseline for all calculations. All differences were considered significant at $P < .05$. All statistical analyses were performed with SAS (SAS Institute), version 9.3, and graphs were created with Prism, version 7.05 (GraphPad Software).

SUPPLEMENTARY REFERENCES

Berardesca E, Lévêque JL, Masson P. European Group for Efficacy Measurements on Cosmetics and Other Topical Products (EEMCO Group). EEMCO guidance for the measurement of skin microcirculation. Skin Pharmacol Appl Skin Physiol 2002;15:442−56.

Borbíró I, Lisztes E, Tóth BI, Czifra G, Oláh A, Szöllosi AG, et al. Activation of transient receptor potential vanilloid-3 inhibits human hair growth. J Invest Dermatol 2011;131:1605−14.

Braun N, Binder S, Grosch H, Theek C, Ülker J, Tronnier H, et al. Current data on effects of long-term missions on the international space station on skin physiological parameters. Skin Pharmacol Physiol 2019;32:43−51.

Cupp MJ, Tracy TS. Dimethylglycine (N,N-dimethylglycine). In: Cupp MJ, Tracy TS, editors. Dietary supplements: toxicology and Clinical Pharmacology. Totowa: Humana Press; 2003. p. 149−60.

Czifra G, Szöllősi AG, Tóth BI, Demaude J, Bouez C, Breton L, et al. Endocannabinoids regulate growth and survival of human eccrine sweat gland-derived epithelial cells. J Invest Dermatol 2012;132:1967−76.

Gascon G, Patterson B, Yearwood K, Slotnick HN. N dimethylglycine and epilepsy. Epilepsia 1989;30:90−3.

Géczy T, Oláh A, Tóth BI, Czifra G, Szöllősi AG, Szabó T, et al. Protein kinase C isoforms have differential roles in the regulation of human sebocyte biology. J Invest Dermatol 2012;132:1988−97.

Greene HM, Wickler SJ, Bray RE, Burrill MJ, London C. The effect of N,N-dimethylglycine on athletic performance at altitude in horses and mules. Pferdeheilkunde 1996;12:499−501.

Kalmar ID, Verstegen MWA, Vanrompay D, Maenner K, Zentek J, Iben C, et al. Efficacy of dimethylglycine as a feed additive to improve broiler production. Livest Sci 2014;164:81−6.

Kendall RV, Glaza SM. Acute oral toxicity (LD_{50}) study in the rat with neutralized N, N-dimethylglycine hydrochloride. J Am Coll Toxicol 1982;1:198.

Klemp P, Lindskov R, Staberg B. Subcutaneous blood flow in alopecia areata. Clin Exp Dermatol 1984;9:181−5.

Lendvai A, Béke G, Hollósi E, Becker M, Völker JM, Schulze Zur Wiesche E, et al. N,N-dimethylglycine sodium salt exerts marked anti-inflammatory effects in various dermatitis models and activates human epidermal keratinocytes by increasing proliferation, migration, and growth factor release. Int J Mol Sci 2023;24:11264.

Markovics A, Angyal Á, Tóth KF, Ádám D, Pénzes Z, Magi J, et al. GPR119 is a potent regulator of human sebocyte biology. J Invest Dermatol 2020;140:1909−1918.e8.

Nagy G, Barcza M, Gonchoroff N, Phillips PE, Perl A. Nitric oxide-dependent mitochondrial biogenesis generates $Ca2^{+}$ signaling profile of lupus T cells. J Immunol 2004;173:3676−83.

Nagy G, Koncz A, Perl A. T cell activation-induced mitochondrial hyperpolarization is mediated by $Ca2^{+-}$ and redox-dependent production of nitric oxide. J Immunol 2003;171:5188−97.

Natarelli N, Gahoonia N, Sivamani RK. Integrative and mechanistic approach to the hair growth cycle and hair loss. J Clin Med 2023;12:893.

Prola L, Nery J, Lauwaerts A, Bianchi C, Sterpone L, De Marco M, et al. Effects of N,N-dimethylglycine sodium salt on apparent digestibility, vitamin E absorption, and serum proteins in broiler chickens fed a high- or low-fat diet. Poult Sci 2013;92:1221−6.

Schulze zur Wiesche E, Becker M, Völker JM, Bussoletti C, Tolaini MV, Celleno L. , 14th−16th June. A novel topical treatment based on sodium dimethylglycinate and caffeine against

malepattern hair loss. Sheffield, UK: 20th EHRS Meeting; 2023.

Swierczynski J, Hebanowska A, Sledzinski T. Serum betaine concentrations and the effects of bariatric surgery. In: Preedy VR, editor. Food and nutritional components in focus. Betaine: chemistry, analysis, function and effects, XX. Cambridge: The Royal Society of Chemistry; 2015. p. 245–66.

Szabó IL, Lisztes E, Béke G, Tóth KF, Paus R, Oláh A, et al. The Phytocannabinoid (-)-cannabidiol Operates as a Complex, Differential Modulator of Human Hair Growth: anti-inflammatory submicromolar versus Hair Growth Inhibitory Micromolar Effects. J Invest Dermatol 2020;140:484–488.e5.

Szöllősi AG, Vasas N, Angyal Á, Kistamás K, Nánási PP, Mihály J, et al. Activation of TRPV3 regulates inflammatory actions of human epidermal keratinocytes. J Invest Dermatol 2018;138:365–74.

Tóth BI, Dobrosi N, Dajnoki A, Czifra G, Oláh A, Szöllosi AG, et al. Endocannabinoids modulate human epidermal keratinocyte proliferation and survival via the sequential engagement of cannabinoid receptor-1 and transient receptor potential vanilloid-1. J Invest Dermatol 2011;131:1095–104.

Tóth BI, Géczy T, Griger Z, Dózsa A, Seltmann H, Kovács L, et al. Transient receptor potential vanilloid-1 signaling as a regulator of human sebocyte biology. J Invest Dermatol 2009;129:329–39.

Walter B, Bauer R, Krug A, Derfuss T, Traichel F, Sommer N. Simultaneous measurement of local cortical blood flow and tissue oxygen saturation by Near infra-red laser Doppler flowmetry and remission spectroscopy in the pig brain. Acta Neurochir Suppl 2002;81:197–9.

Wolfsegger T, Böck K, Schimetta W, von Oertzen TJ, Assar HN. N-dimethylglycine in patients with progressive multiple sclerosis: result of a pilot double-blind, placebo, controlled randomized clinical trial. Neurol Res Pract 2021;3:29.

Supplementary Table S1. Dermal Blood Flow between 0 and 90 Minutes after Verum or Placebo Application and Untreated Control at 1-mm Skin Depth

	Flow (1 mm)				Pre–Post Difference in Flow (1 mm)		
Groups	**0 min**	**30 min**	**60 min**	**90 min**	**ΔT30**	**ΔT60**	**ΔT90**
Verum	6.8 ± 2.72	7.18 ± 7.51	8.48 ± 6.67	7.85 ± 4.12	0.39 ± 7.48	1.68 ± 6.77[1]	1.05 ± 4.16[1]
Placebo	8.58 ± 3.60	7.99 ± 7.43	7.20 ± 4.85	6.91 ± 3.59	−0.59 ± 8.15	−1.38 ± 5.23	−1.67 ± 5.17
Untreated control	9.87 ± 6.75	6.06 ± 2.40	6.44 ± 3.34	7.54 ± 5.48	−3.80 ± 5.47	−3.42 ± 5.39	−2.32 ± 4.81

Values are presented as mean ± SD (n = 20).
[1]$P < .01$ denotes significant difference compared with the untreated control.

Supplementary Table S2. Dermal Blood Flow between 0 and 90 Minutes after Verum or Placebo Application and Untreated Control at 8-mm Skin Depth

	Flow (8 mm)				Pre–Post Difference in Flow (8 mm)		
Groups	**0 min**	**30 min**	**60 min**	**90 min**	**ΔT30**	**ΔT60**	**ΔT90**
Verum	32.96 ± 11.52	39.83 ± 29.76	34.74 ± 14.58	40.47 ± 20.66	6.86 ± 28.58[1]	1.77 ± 13.16[1]	7.51 ± 16.86[2,3]
Placebo	43.58 ± 18.92	39.85 ± 18.92	39.60 ± 21.82	36.89 ± 20.46	−3.73 ± 14.09	−3.98 ± 12.15	−6.69 ± 14.55
Untreated control	44.25 ± 14.83	34.78 ± 11.71	35.34 ± 12.17	34.91 ± 13.14	−9.47 ± 10.69	−8.91 ± 10.31	−9.34 ± 9.90

Values are presented as mean ± SD (n = 20).
[1]$P < .01$ denotes significant difference compared with the untreated control.
[2]$P < .01$ denotes significant difference compared with the placebo.
[3]$P < .001$ denotes significant difference compared with the untreated control.

Supplementary Table S3. Dermal Blood Velocity between 0 and 90 Minutes after Verum or Placebo Application and Untreated Control at 1-mm Skin Depth

	Velocity (1 mm)				Pre–Post Difference in Velocity (1 mm)		
Groups	**0 min**	**30 min**	**60 min**	**90 min**	**ΔT30**	**ΔT60**	**ΔT90**
Verum	10.53 ± 1.26	11.52 ± 5.98	11.47 ± 5.09	11.07 ± 1.63	0.99 ± 5.5	0.95 ± 4.57[1]	0.54 ± 1.30[2,3]
Placebo	11.02 ± 1.82	11.72 ± 6.01	10.74 ± 3.65	10.44 ± 2.22	0.70 ± 6.36	−0.28 ± 2.58	−0.58 ± 1.91
Untreated control	11.69 ± 3.81	10.10 ± 1.93	10.25 ± 2.07	10.94 ± 2.26	−1.59 ± 2.84	−1.44 ± 2.77	−0.75 ± 2.32

Values are presented as mean ± SD (n = 20).
[1] $P < .05$ denotes significant difference compared with the untreated control.
[2] $P < .05$ denotes significant difference compared with the placebo.
[3] $P < .01$ denotes significant difference compared with the untreated control.

Supplementary Table S4. Dermal Blood Velocity between 0 and 90 Minutes after Verum or Placebo Application and Untreated Control at 8-mm Skin Depth

	Velocity (8 mm)				Pre–Post Difference in Velocity (8 mm)		
Groups	**0 min**	**30 min**	**60 min**	**90 min**	**ΔT30**	**ΔT60**	**ΔT90**
Verum	13.75 ± 2.04	14.89 ± 4.45	13.94 ± 2.55	14.46 ± 2.81	1.15 ± 4.92[1,2]	0.20 ± 2.53[2]	0.72 ± 2.42[3,4]
Placebo	14.74 ± 3.64	13.63 ± 3.35	13.77 ± 4.02	13.41 ± 3.56	−1.11 ± 2.79	−0.97 ± 2.85	−1.33 ± 2.76
Untreated control	15.47 ± 3.58	13.64 ± 2.61	13.48 ± 2.62	13.71 ± 2.81	−1.84 ± 2.05	−2.00 ± 1.66	−1.76 ± 1.75

Values are presented as mean ± SD (n = 20).
[1] $P < .05$ denotes significant difference compared with the placebo.
[2] $P < .05$ denotes significant difference compared with the untreated control.
[3] $P < .01$ denotes significant difference compared with the placebo.
[4] $P < .01$ denotes significant difference compared with the untreated control.